Comparative Medicine
Copyright 2014
by the American Association for Laboratory Animal Science

Vol 64, No 5
October 2014
Pages 377–385

*Original Research*

# Ovine Model for Critical-Size Tibial Segmental Defects

**Chris Christou,* Rema A Oliver, Matthew H Pelletier, and William R Walsh**

**A segmental tibial defect model in a large animal can provide a basis for testing materials and techniques for use in nonunions and severe trauma. This study reports the rationale behind establishing such a model and its design and conclusions. After ethics approval of the study, aged ewes (older than 5 y; *n* = 12) were enrolled. A 5-cm mid diaphyseal osteoperiosteal defect was made in the left tibia and was stabilized by using an 8-mm stainless-steel cross-locked intramedullary nail. Sheep were euthanized at 12 wk after surgery and evaluated by using radiography, microCT, and soft-tissue histology techniques. Radiology confirmed a lack of hard tissue callus bridging across the defect. Volumetric analysis based on microCT showed bone growth across the 16.5-$cm^3$ defect of 1.82 ± 0.94 $cm^3$. Histologic sections of the bridging tissues revealed callus originating from both the periosteal and endosteal surfaces, with fibrous tissue completing the bridging in all instances. Immunohistochemistry was used to evaluate the quality of the healing response. Clinical, radiographic, and histologic union was not achieved by 12 wk. This model may be effective for the investigation of surgical techniques and healing adjuncts for nonunion cases, where severe traumatic injury has led to significant bone loss.**

**Abbreviations:** BMP2, bone morphogenic protein 2; CATK, cathepsin K; VEGF, vascular endothelial growth factor.

The human tibia is the most frequently broken long bone, often with significant bone loss.[4] Segmental tibial defects can occur as a result of large tumor removal, trauma such as motor vehicle accidents, and more recently, blast injuries as seen with the escalating number of global conflicts. Treatment of these large bone and surrounding soft tissue defects is an ongoing, costly, and challenging clinical problem; no surgical technique has currently achieved preeminence.[4] The general consensus on factors that affect healing include concomitant disease, age, and degree of trauma.[5] When the first 2 factors, which are patient-related, are removed from the equation, healing is influenced by the size, anatomic location, and soft-tissue coverage of the defect. The ability to study these situations in a well-controlled, robust, and reproducible preclinical model would be advantageous to help establish effective surgical techniques and evaluate implants and materials.

A literature review revealed that many ovine models for bone defects have been used, but all have limitations[6,12,14,15,20,21,24,25,27,31,37,39,40] (Figure 1). Variations in protocols, such as age of the animals, size of the defect, and the bone and stabilization techniques used, limit meaningful comparison between studies.[33,34] Although some studies have investigated material performance in the healing of defects, they did not rigorously quantify control defects,[17,20] and others used no controls at all.[39] There is often no explanation regarding the use of a particular defect size, leading to the question of whether the defect size was critical.[24] The choice of bone used has been also varied; the femur,[15] tibia,[37] and metatarsus[40] have all been studied. A noncritical-size defect implies that healing would eventually occur without the presence of any graft materials. One study,[12] for example, used a 3-cm defect at an average of 1.8 times the diameter of the tibias in question and found that empty controls achieved as much as 26% of the stiffness of an intact tibia after 12 wk. Stabilization methods include plating,[21,40] external fixtures,[20] intramedullary nails,[6,16] and a combination of intramedullary nails and plating.[37]

The criteria used in the present study for a critical-size segmental tibial defect model were based on the following factors. The ovine tibia closely resembles that of the human tibia in terms of size, shape, and physical properties and is commonly used when studying human orthopedic diseases.[26,34] Intramedullary nailing has become the most commonly used method of tibial fracture fixation in human orthopedic surgery.[8,22] An 8-mm intramedullary nail is commonly used in the treatment of human fractures, further confirming the size similarity between the ovine and human tibiae.[19]

The aim of this study was to establish and characterize a preclinical ovine 5-cm osteoperiosteal critical-size tibial segmental defect model in mature sheep. The endpoints included those commonly used clinically, such as radiography and microCT. Histology to investigate the degree of healing and immunohistochemistry to characterize the healing process were included to complete the evaluation process.

## Materials and Methods

Ethics approval was gained from the Animal Care and Ethics Committee of the University of New South Wales. Adult crossbred ewes (*n* = 12; age, 5 to 6 y; weight, 55 ± 5 kg) were divided

*Received: 19 Feb 2014. Revision requested: 19 Apr 2014. Accepted: 16 May 2014.*
*Surgical and Orthopaedic Research Laboratory, Prince of Wales Clinical School, University of New South Wales. Avoca St Randwick, Australia.*
**Corresponding author. Email: c.christou@unsw.edu.au*

| Bone | Defect size | Age | Sex | Fixation |
|---|---|---|---|---|
| Tibia[32] | 5cm | "Skeletally mature" | Female | IM nail |
| Tibia[12] | 3cm | Age not mentioned | Female | IM nail |
| Metatarsus[41] | 2.5cm | 2yrs | Female | Plate/Cast |
| Tibia[14] | 3cm | 4yrs | Female | IM nail |
| Femur[15] | 5cm | 3yrs | Male | IM nail |
| Tibia[40] | 3.5cm | 4-5mths | Male/Female | Plate |
| Tibia[20] | 4cm | Age not mentioned | Female | Double Ex Fix |
| Tibia[21] | 3cm | "Skeletally mature" | Female | Double Plate |
| Tibia[24] | 1.8cm | 4-5yrs | Female | Single Ex Fix |
| Tibia[25] | 3.5cm | 2yrs | Female | Single Ex Fix |
| Tibia[38] | 2.5cm | 5-7yrs | Female | Plate/Nail Hybrid |
| Tibia[28] | 4.8cm | 2yrs | Female | Plate/Cast |
| Tibia[6] | 3cm | 2yrs | Female | IM nail |

**Figure 1.** A limited summary of the many studies where a segmental tibial has been used with their references.

into pairs and acclimated in their respective stalls (6 $m^2$) for 1 wk prior to surgery. They were maintained on a diet of lucerne hay, chaff, and water ad libitum.

Each sheep was given preemptive analgesia 72 h prior to surgery by using a transdermal fentanyl (100 µg) patch (Durogesic, Janssen, Sydney, Australia). Twelve hours prior to surgery, all food was removed from the stalls. On the day of surgery, the fentanyl patch was replaced to provide another 72 h of analgesia postoperatively.[1,2] After sedation with tiletamine–zolazepam (5 mg/kg; Zoletil, Virbac Animal Health, Sydney, Australia) and gaseous anesthetic mask induction with isoflurane (Abbott, Sydney, Australia), an 8-mm endotracheal tube was placed and the cuff inflated. Anesthesia was maintained with isoflurane. The left hindlimb was clipped and aseptically prepared for surgery. An 18-gauge intravenous catheter was placed in the left cephalic vein, and a 1-L bag of Hartman solution was attached and infused at a rate of 1.5 times maintenance. Long-acting oxytetracycline (10 mg/kg IM; Troy Ilium, Sydney, Australia) carprofen (2 mg/kg IV;

**Figure 2.** Marking of the tibia intraoperatively before the 5-cm osteotomy. The arrow indicates the point where the tibial crest meets the diaphysis.

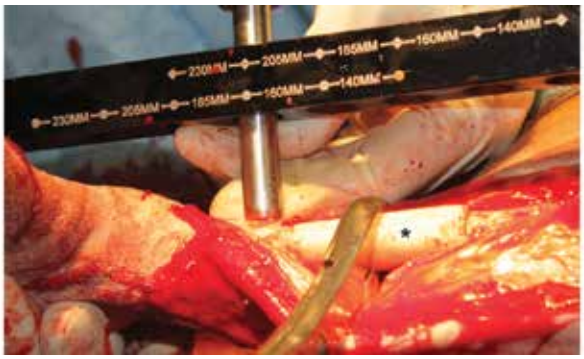


**Figure 3.** After the osteotomy, the bone segment (asterisk) is held in place to maintain gap length while the distal segment is being drilled for the cross-locking bolts.

Rimadyl, Pfizer, Sydney, Australia), and cephalexin (20 mg/kg IV; Virbac Animal Health) were provided.

Each sheep was placed in dorsal recumbency, and a craniomedial approach to the tibia was used. The midshaft of the left tibia was exposed and identified as a point 20 mm from where the ridge of the tibial crest flattens and meets the tibial diaphysis (Figure 2). Measuring 25 mm proximal and distal to this point, a 50-mm section of the diaphysis and its associated periosteum was removed by using a saline-cooled oscillating saw (Microaire, Zimmer, Sydney, Australia). The size of each medullary cavity encountered was such that only 0.5 to 1 mm of reaming was required to reach the desired 8-mm medullary cavity diameter. The tibia was stabilized and returned to its original length and orientation by using an stainless steel intramedullary nail (diameter, 8 mm; length, 185 mm) and 2 proximal and 2 distal 4.5-mm cross-locking bolts (Innovative Animal Products, Rochester, MN). At the time of nail locking, the piece of bone that was removed was split in half longitudinally and placed across the defect to maintain the correct spacing (Figure 3). The defect was left empty, and the surrounding tissues closed in their respective layers. Postoperative radiographs were taken immediately.

The sheep were returned to their stalls and monitored by a veterinarian for pain every 12 h during the 72-h period postoperatively. Criteria used included degree of lameness, appetite, and general overall demeanor of each animal. After the acute postoperative period, the sheep were monitored every 12 h by the animal technicians, who observed the sheep's appetite and demeanor. Postoperative husbandry was kept simple, free movement was allowed, the sheep were kept in pairs for socialization, visual contact across the pens was maintained, and nonslip bedding

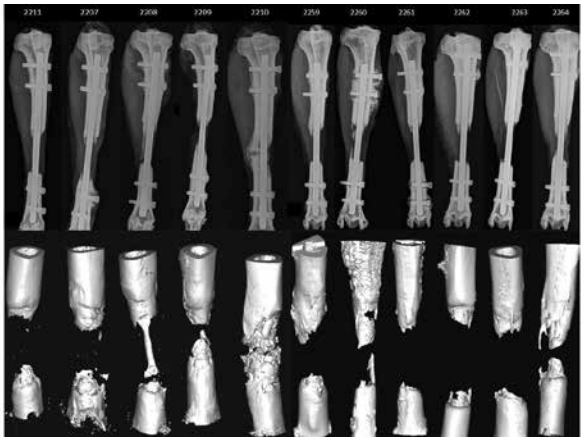

**Figure 4.** Anteroposterior Faxitron radiographs at 12 wk and their corresponding 3D models extracted from the microCT data demonstrate the incomplete bridging of the defects. Due to cropping, not all the radiographs are to scale; the reference point is that every nail is 8 mm in diameter.

was provided. There was no need for harnessing or any other form of weight support; all sheep were euthanized at 12 wk.

Limb usage was monitored and evaluated daily as an assessment of pain. The following classification system was devised for use in this study: 5, nonweightbearing; 4, occasional placement of leg; 3, use of leg when walking but not when standing still; 2, nearly fully weightbearing when walking and resting on the leg when still; 1, normal weightbearing. All observations were recorded on each animal's daily postoperative monitoring sheet.

At the time of euthanasia all tibias were harvested, and Faxitron radiographs (Faxitron Tucson, AZ) in the lateral and anteroposterior planes were taken by using digital plates (Agfa, Scoresby, Victoria, Australia) and with the intramedullary nail in situ. The radiographs were graded according to the amount of callus tissue bridging the defect site in a blinded fashion by 2 independent observers who used the following scale: grade 1, 0% to 25%; grade 2, 25% to 50%; grade 3, 50% to 75%; and grade 4, 75% to 100%. The distance across each defect was measured to check the integrity of the defect gap after 12 wk, and the bony callus was measured at its longest distance from osteotomy site to the middle of the defect from both the proximal and distal ends of the defect by using the radiographic images and Image J software (version 1.44, NIH, Bethesda, MD).

The intramedullary nails were removed from each tibia by removing the cross-locking bolts prior to cutting the tibia just below the tibial plateau. To avoid beam artifact during the microCT scanning,[7] the nail was removed carefully so as not to disturb any callus at the defect site. Four-bed microCT scans (Inveon Siemens, Erlangen, Germany) to include the whole tibia were performed at 80 kV, 500 µA, with a resolution (pixel size) of 54 µm. The data were imported into Mimics software (Materialise, Leuven, Belgium) for analysis. All images were thresholded to remove any soft tissue and cartilage, leaving only bone. The thresholding was performed visually based on the removal of the existing soft-tissue densities present on the tibia at the time of scanning; consistent grayscale values were used. 3D images were constructed and sectioned to isolate the defect site. The volume of bony tissue filling the defect site was calculated from the 3D models produced by using Mimics software.

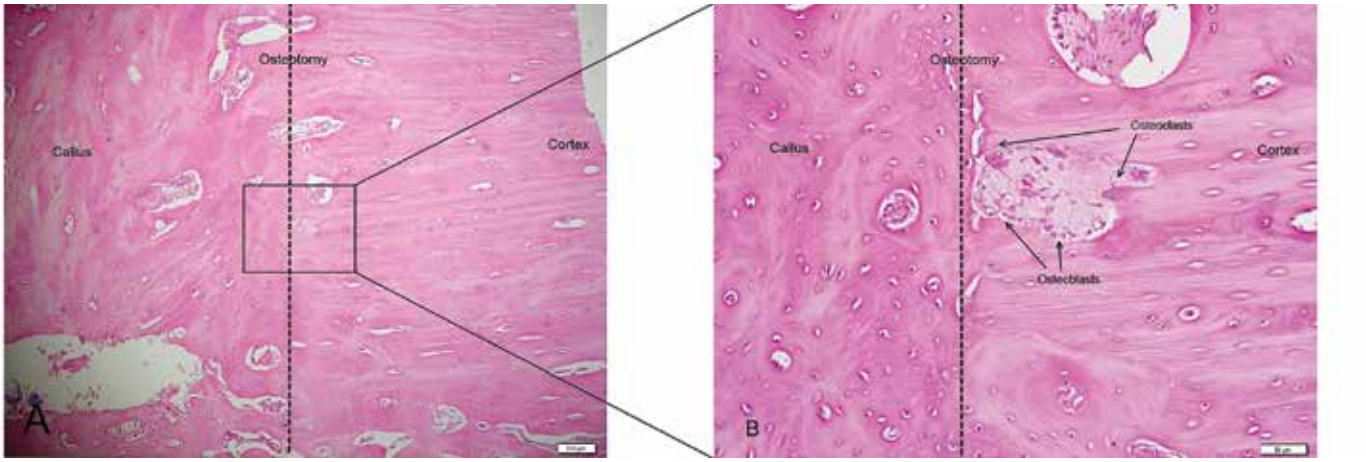


**Figure 5.** (A) Callus growth at the osteotomy. Magnification, 40×. (B) A magnified view from inside the square, showing osteoblasts and osteoclasts around the site of the osteotomy where the callus is docking with the cortical bone and where remodeling has begun. Magnification, 200×.

The tibias were decalcified in 10% formic acid in PBS. The bones were cut through the middle of the defect in 2 planes, one parallel to the long axis of the tibia to produce coronal sections, and the other perpendicular to it, giving proximal and distal sections. The tissues were processed for paraffin histology, and 4 × 5-µm sections were cut from each block by using a microtome (Leica MicroSystems, Wetzlar, Germany). Sections were stained with Harris hemtoxylin and eosin for cellular staining and identification and modified tetrachrome for tissue differentiation of osteoid, mature lamellar bone, woven bone, mineralization of front cartilage, and calcified cartilage.[32] Cellular type and position within the healing tissues were assessed for each slide from 6 high-power fields (magnification, 400×) viewed at 3 points within the callus: close to the osteotomy and the middle and distal areas.

Standard immunohistochemical procedures were performed on all 5-µm paraffin sections for expression of cathepsin K (CATK), ALP, bone morphogenic protein (BMP2), vascular endothelial growth factor (VEGF), TGFβ, and IL6.[42] After deparaffinization, heat-based antigen recovery was performed on the tissues by using a citrate-based solution (DAKO, Glostrup, Denmark) at 100 °C for 30 min. Endogenous peroxidase was quenched in 0.3% hydrogen peroxide in 50% methanol for 10 min followed by a rinse in 0.01% Tween 20 in PBS. Primary mouse monoclonal antibodies against CATK (0.1µg/mL; Santa Cruz Biotechnology, Dallas, TX), ALP (0.5 µg/mL; Santa Cruz Biotechnology), BMP2 (2 µg/mL; Santa Cruz Biotechnology), VEGF (5 µg/mL; Santa Cruz Biotechnology), and IL6 (2 µg/mL; Santa Cruz Biotechnology) were used, with nonimmunized mouse IgG (5 µg/mL, Dako) as a negative control. Primary rabbit monoclonal antibodies against TGFβ (4 µg/mL; Santa Cruz Biotechnology) were used with nonimmunized rabbit IgG (4µg/mL; Dako) as a negative control The slides were incubated overnight at 4 °C, washed with Tween 20 in PBS, and incubated with HRP-labeled polymer (antimouse K4001, Dako Cytomation, Carpinteria, CA) for 1 h. After the slides were washed with Tween 20 in PBS, a substrate–chromogen system (catalog no. K24668, liquid diaminobenzidine, Dako) was applied for 30 min. The reaction was stopped by rinsing in PBS, slides were counterstained by using Harris hematoxylin, and coverslips were mounted. Each slide was analyzed under light microscopy for protein expression.

## Results

During the immediate postoperative period, all sheep appeared comfortable, stood and sat with relative ease, and had normal appetite, indicating the effectiveness of the fentanyl patches. No additional analgesia was required. All soft-tissue wounds healed, well and no additional antibiotics were required. Across all sheep, weightbearing immediately postoperatively was evaluated as grade 3, according to the aforementioned scale. All sheep achieved a grade 2 ambulation score by week 3. On the 21st postoperative day, one sheep was discovered to be unwilling to stand, and additional investigation revealed a fracture below the defect site. The sheep was euthanized, the tibia was radiographed, and gross dissection showed that the problem was due to failure of the intramedullary nail at the proximal hole of the 2 distal cross-locking bolts.

The remaining 11 sheep remained on study until the intended 12-wk time point. Of these 11 sheep, 3 showed slight reduction in limb usage during the final 3 wk of the study, such that their lameness scores were 2 or 3 instead of 2. Clinical examination revealed minor instability, with no loss of integrity of the overall nail–tibia construct and no associated pain.

At the time of tissue harvest, 1 sheep (no. 2260) had a mild infection at the proximal locking bolts (Figure 4). At no stage did this animal show signs of lethargy or inappetence, and its skin and the surrounding tissues showed no premortem evidence of infection.

Plain-film radiographs and microCT showed the initiation of a callus reaction at all cut bony edges, indicating that all defects had some initial attempt at healing (Figure 4). All cases showed failure of union between the 2 healing ends of the bone, as demonstrated by the lack of any significant hard tissue in the defect region; only a fibrous union was present. According to the aforementioned grading scale, 9 tibias were classed as grade 1 (0% to 25%) relative to the amount of callus forming across the gap, 1 was grade 2 (25% to 50%), and 1 was a grade 4 (75% to 100%). The defect sizes, as measured at 12 wk, ranged from 44 to 50 mm in length (mean ± 1 SD, 47.8 ± 1.9 mm). The absolute distances across the defect site produced a span of 24.7 ± 10.3 mm. This value excludes the tibia in which bridging was almost complete, because the gap could not be measured from the radiograph. Four tibias (sheep 2207, 2210, 2260, and 2261) had loosening of a cross-locking bolt at the

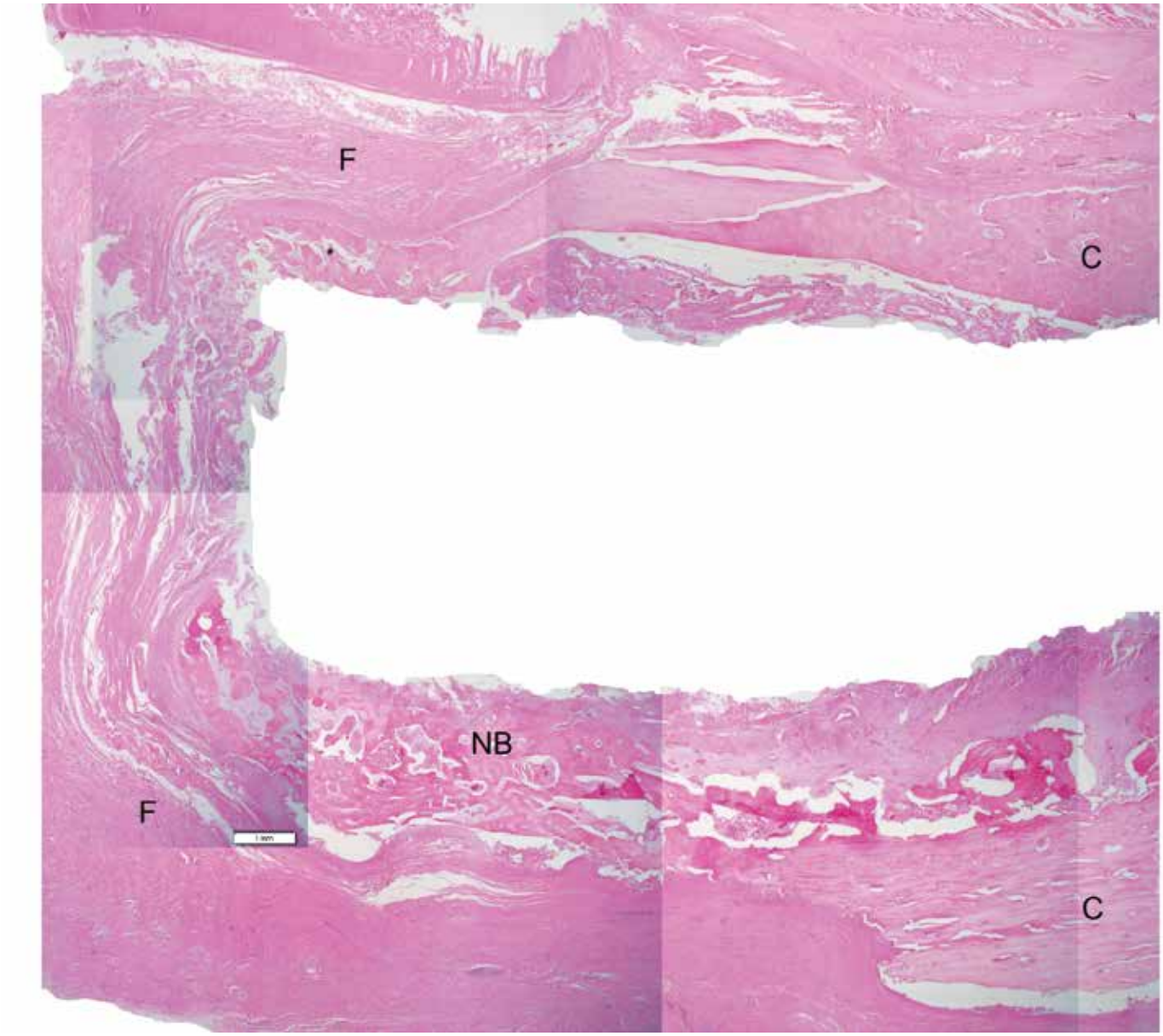


**Figure 6.** A composite image generated from multiple slide shots of a slide section across the defect that shows the nonunion. C, cortex; F, fibrous tissue; NB, new bone growth. Magnification, 12.5×.

time of harvest, as noted on radiographs (Figure 4). These sheep were the same ones that showed a decrease in leg usage during the last 3 wk of the study.

MicroCT further confirmed the radiographic findings and provided the added benefit of volumetric analysis (Figure 4). Given an external diameter of 22 mm and an internal diameter of 8 mm (as reamed during surgery), the amount of bone that is needed to fill a 50-mm defect is 16.5 $cm^3$. The volume of bone that grew across the gap in the 11 sheep was 2.55 ± 2.54 $cm^3$. The grade 4 tibia had 9.76 $cm^3$ of bone bridging the defect and thus caused the relatively large SD. Omitting this tibia from the calculations led to a volume of 1.83 ± 0.94 $cm^3$ of bone that grew across the gap. In all cases, the bone originated from the osteotomy site both proximally and distally; there appeared to be no spontaneous intramembranous bone formation in the middle of the callus.

Histologic evaluation of the defect site reflected an active healing process at 12 wk (Figure 5). Hematoxylin and eosin staining revealed the presence of osteoclasts and osteoblasts close to the osteotomy site, confirming active bone remodeling after callus initiation. Further into the callus, osteoblasts were present on the surfaces of the newly formed bone, and few osteoclasts were found, indicating an anabolic process with little remodeling. Nonunion was still evident at the extremities of all calluses (Figure 6).

Strong staining for ALP was seen at all bone edges within and around the advancing callus, demonstrating osteoblastic activity (Figure 7 A). Weak CATK staining occurred in the areas of the initial callus adjacent to the osteotomy site (Figure 7 B), confirming the presence of osteoclastic activity where remodeling would be expected to begin. No cellular staining for CATK is visible at the edges of the newly formed advancing callus (Figure 7 B).

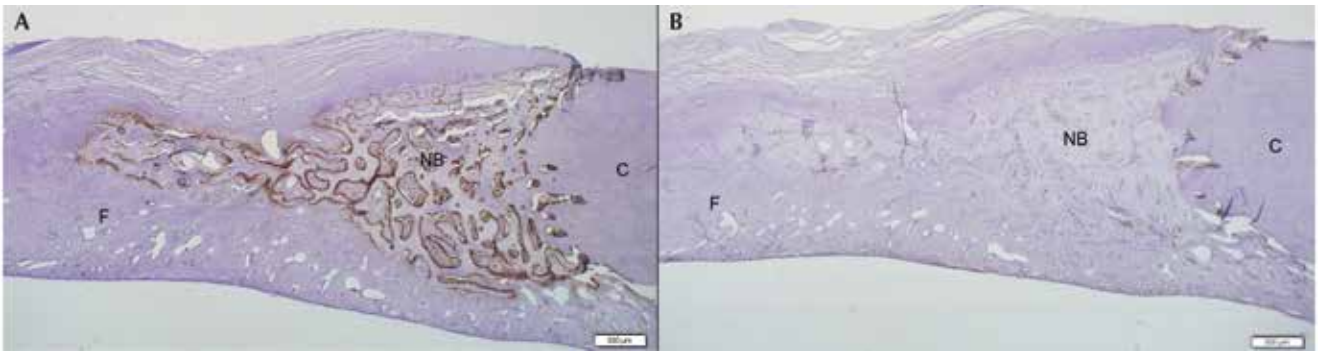


**Figure 7.** Immunohistochemistry of the slide section shown in figure 6. (A) Alkaline phosphatase stain. (B) CAT-K stain. See Table 1. C, cortex; F, fibrous tissue; NB, new bone growth. Magnification, 20× .

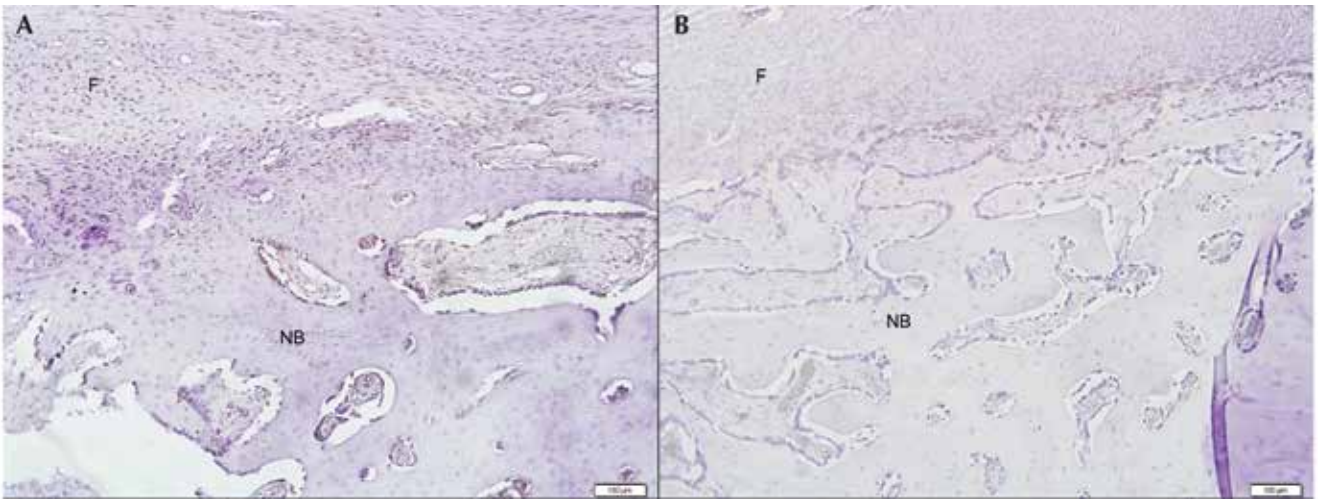


**Figure 8.** Weak to mild expression of (A) BMP2 and (B) VEGF at an advancing edge within a callus at 12 wk. See Table 1. NB, new bone; F, fibrous tissue. Magnification, 100×.

BMP2, VEGF, and TGF-β were all found within the callus tissues. BMP2 and VEGF (Figure 8 A and B) were closely associated with the osteoblasts present in the callus. Their signals however were weak and not present on every osteoblast. TG-β was found in the fibrous tissues as far as 1 mm away from the cells that stained for BMP2 and VEGF within the callus (Figure 9). Staining for IL6 was negative in all slides (Table 1).

## Discussion

The establishment of a standardized, preclinical, critical-size segmental defect model in a large animal will assist in the development and improvement of treatment modalities for cases of critical bone loss, To date, it has been difficult to achieve such a model.[23] Many factors play a role in such model development, including the choice of species, sex, age, anatomic location, and choice of fixation method.

According to the breed of sheep we used in our study (first-generation merino crossbreds), the ovine tibia has an average midshaft diameter of 22 mm. Research has shown that for a defect to be critically sized, its length must exceed 2 to 2.5 times the diameter of the bone in question.[12,34] From this, a 50-mm defect was deemed an appropriate size. Ewes older than 5 y were chosen to better represent a skeletally mature adult, with bone changing from lamellar to Haversian in structure from 4 y of age onward and therefore more closely resembling that of human

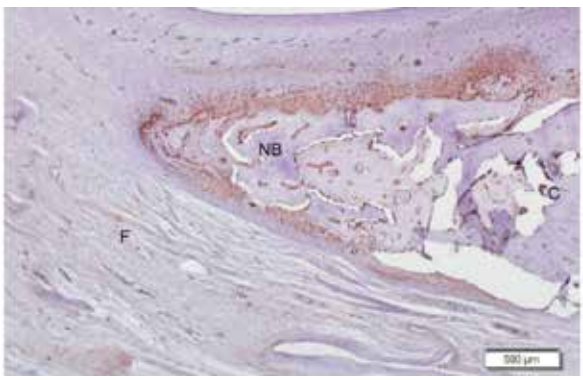


**Figure 9.** Strong TGFβ expression advancing into the surrounding fibrous tissue at 12 wk. Magnification, 40×.

bone.[29] Many previous studies only mention the use of adult or skeletally mature sheep; this wording merely indicates an animal older than 18 mo, and the bone is still lamellar and thus more rapidly growing in these younger sheep.[12,20,21] In addition, compared with mature adults, younger sheep have a greater healing capacity, one more closely related to that of the adolescent skeleton than the adult skeleton in humans.[26] An expected time to union of a simple fracture in sheep is 10 to 14 wk;[28] accordingly a 12-wk endpoint was chosen to harvest the tissues for examination of the healing response.

**Table 1.** Staining intensity of the immunohistochemical factors tested (no staining to strong staining, – to +++)

| Animal | ALP | CATK | BMP2 | VEGF | TGFβ | IL6 |
|---|---|---|---|---|---|---|
| 2207 | +++ | + | + | ++ | ++ | — |
| 2208 | +++ | ++ | ++ | ++ | +++ | — |
| 2209 | +++ | + | ++ | ++ | +++ | — |
| 2210 | +++ | + | +++ | +++ | +++ | — |
| 2211 | +++ | + | ++ | ++ | +++ | — |
| 2259 | +++ | + | + | ++ | ++ | — |
| 2260 | +++ | ++ | + | ++ | +++ | — |
| 2261 | +++ | + | + | ++ | ++ | — |
| 2262 | +++ | +++ | ++ | ++ | +++ | — |
| 2263 | +++ | ++ | ++ | ++ | +++ | — |
| 2264 | +++ | ++ | +++ | ++ | +++ | — |

The choice of fracture fixation method is influenced by the nature of the injury as well as load-bearing considerations. Intramedullary nailing was chosen in the current study because it has become the fixation method of choice for diaphyseal fractures of long bones in humans.[36] Intramedullary nailing is a mechanically superior fixation method when compared with plating in load-bearing bones such as the tibia.[3,9] The implant lies in the plane of axial loading, producing a more efficiently placed area moment of inertia when compared with that of an eccentrically placed plate. Greater implant bone contact surface area also reduces the stress points on the bone when compared with the smaller contact area associated with plating.[10] The eccentric placement of plates relative to the axial forces requires the plates to be stiffer to resist weight-bearing forces, therefore they are associated with stress shielding of the fracture site and can place pressure on the periosteum, compromising blood supply. In one study,[33] plate failure was noted associated with a 3-cm defect in sheep, thus demonstrating a potential limitation of such devices. In addition, the presence of an intramedullary nail at the defect reduces the amount of graft material required; the nail acts as space filler, serves as a potential guide for tissue growth, and provides for the formation of a medullary cavity during the healing process. Intramedullary nailing can be performed in a closed fashion.

The results presented here indicate that despite one sheep achieving bone filling of 9.76 $cm^3$ across the defect site, radiography, microCT, and histology all confirmed that none of the 11 sheep evaluated at the 12-wk point achieved union of a critical-size tibial defect. The dramatic healing response of the remaining sheep highlights the variability that can occur in live animal models. The benefit of using microCT in conjunction with radiography is that microCT more accurately assesses not only the amount of bone bridging the defect but also the quality of bone growth. Although not available clinically, histology and immunohistochemistry provided useful insight regarding the bone's healing response and its progress.

Histology allowed for the identification of tissue types present in the callus, confirming the delayed unions seen in the imaging. Immunohistochemistry was useful in confirming the continued anabolic nature of the distal callus at its advancing edge. The presence of ALP at the advancing edges of the callus is indicative of an active mineralization process at the callus margins.[18] This feature in combination with weak and sporadic BMP2 and VEGF staining, which work synergistically in endothelial cell and osteoblast maturation and metabolism,[11] combine to indicate that although the healing response was not exhausted, the nature and size of the defect exceeded the body's natural healing capacity at the given postoperative time point. The role of TGFβ within tissues is dependent on the surrounding environment.[41] In this series of animals, the presence of TGFβ appears to be as a primer of tissue differentiation prior to the influx of tissue factors such as BMP2 and VEGF.[35] Catabolic processes were investigated by staining for CATK and IL6. CATK is a cysteine protease released from osteocytes that are cleaving collagen and degrading bone matrix and is critical in bone resorption and remodeling.[38] The weak CATK staining in the callus adjacent the osteotomy sites indicates that despite delayed healing and lack of mechanical stimulation, callus remodeling was occurring. The negative IL6 staining was useful in confirming that chronic inflammation was not present across the defect site.

Segmental tibial defects of 30 mm in sheep have been reported where the empty defects were bridged by tissues that provided some inherent stability to the tibia.[12] Mechanical testing of the empty defects showed as much as 26% of the torsional stiffness of an intact tibia at 12 wk postoperatively, indicating probable progression to union; therefore the defects cannot be classified as critically sized.[6,13] A study involving a 50-mm tibial defect did not mention the age of the sheep, only stating that they were skeletally mature.[31] Skeletal maturity can occur as young as 18 mo and therefore does not allow for the slow conversion from lamellar to Haversian bone and the reduced healing capacity of the older animal. Furthermore a less challenging healing environment was established by not removing the periosteum at the time of surgery, leading to increased bone regrowth capacity.[31] In another study, 48-mm tibial defect was created, but the surgery was performed on young 2-y-old sheep, no controls were used, and some periosteum was left as a source of healing cells.[27] Although the femur can be a good candidate for a critical-size defect model, its surrounding muscle makes the surgical approach more demanding than that for the tibia.[15] In addition, the muscle reduces the severity of the healing conditions in the femur by providing good soft-tissue coverage, collateral blood supply, and a possible source of muscle-derived stem cells,[30] when compared with the relative lack of soft tissue coverage in the tibia.

A single time point, 12 wk, was used in the current study. Although additional time points and animals would have been advantageous, considering the status of the defects as indicated by radiographic and histology parameters, union at later points was possible, although unlikely. The aim of the present study was to characterize the heal-

ing capacity of sheep with a 5-cm osteoperiosteal defect at a 12-wk time point to provide a basis for the testing of implant materials and surgical techniques used in the healing of bony defects in the harshest of environments. The current study has provided, in a logical progression, the reasoning behind the choices made in establishing this preclinical, critical-size defect model in sheep.

A limitation to this study is the fact that 4 of the 12 animals had some loosening of the cross-locking bolts by the 12-wk time point. The one sheep that had significantly more callus formation than did the others highlights the variability that can be experienced in live animal model studies. Despite the excellent healing response, microCT was useful in confirming a delayed union in this animal (Figure 4: 2210). Interestingly, this sheep had slight loosening of the proximal-most of the proximal 2 bolts, whereas the loosening that occurred in the other sheep happened either at the distal bolts or, in the case of sheep 2260, both proximal bolts. The bolt loosening for 2210 was only evident at harvest; clinically the animal showed no indication of nail loosening.

A sample of one does not provide any conclusive evidence, but it allows for interpretation and formulation of a hypothesis. For example, did the partial dynamization from the proximal loosening of the cross-locking bolts promote callus formation in the animal with grade 4 healing?

## Acknowledgments

We thank John Rawlinson, Greg Mitchell, and Shane Mcgufficke for their assistance with this study.

## References

1. **Ahern BJ, Soma LR, Boston RC, Schaer TP.** 2009. Comparison of the analgesic properties of transdermally administered fentanyl and intramuscularly administered buprenorphine during and following experimental orthopedic surgery in sheep. Am J Vet Res **70:**418–422.
2. **Ahern BJ, Soma LR, Rudy JA, Uboh CE, Schaer TE.** 2010. Pharmacokinetics of fentanyl administered transdermally and intravenously in sheep. Am J Vet Res **71:**1127–1132.
3. **Bernarde A, Diop A, Maurel N, Viguier E.** 2001. An in vitro biomechanical study of bone plate and interlocking nail in a canine diaphyseal femoral fracture model. Vet Surg **30:**397–408.
4. **Bhandari M, Guyatt GH, Tornetta P, Swiontkowski MF, Hanson B, Sprague S, Syed A, Schemitsch EH.** 2002. Current practice in the intramedullary nailing of tibial shaft fractures: an international survey. J Trauma **53:**725–732.
5. **Bhandari M, Tornetta P, Sprague S.** 2003. Predictors of reoperation following operative management of fractures of the tibial shaft. J Orthop Trauma **17:**353–361.
6. **Blokhuis TJ, Wippermann BW, den Boer FC, van Lingen A, Patka P, Bakker FC, Haarman HJ.** 2000. Resorbable calcium phosphate particles as a carrier material for bone marrow in an ovine segmental defect. J Biomed Mater Res **51:**369–375.
7. **Boas FE, Fleischmann D.** 2012. CT artifacts: causes and reduction techniques. Imaging Med **4:**229–240.
8. **Bong MR, Kummer FJ, Koval KJ, Egol KA.** 2007. Intramedullary nailing of the lower extremity: biomechanics and biology. J Am Acad Orthop Surg **15:**97–106.
9. **Burns CG, Litsky AS, Allen MJ, Johnson KA.** 2011. Influence of locking bolt location on the mechanical properties of an interlocking nail in the canine femur. Vet Surg **40:**522–530.
10. **Chao P, Lewis DD, Kowaleski MP, Pozzi A.** 2012. Biomechanical concepts applicable to minimally invasive fracture repair in small animals. Vet Clin North Am Small Anim Pract **42:**853–872.
11. **Deckers MML, Karperien M, van der Bent C, Yamashita T, Papapoulos SE, Löwik CWGM.** 2000. Expression of vascular endothelial growth factors and their receptors during osteoblast differentiation. Endocrinology **141:**1667–1674.
12. **den Boer FC, Patka P, Bakker FC, Wippermann BW, van Lingen A, Vink GQ, Boshuizen K, Haarman HJ.** 1999. New segmental long bone defect model in sheep: quantitative analysis of healing with dual energy X-ray absorptiometry. J Orthop Res **17:**654–660.
13. **den Boer FC, Wippermann BW, Blokhuis TJ, Patka P**. 2003. Healing of segmental bone defects with granular porous hydroxyapatite augmented with recombinant human osteogenic protein-1 or autologous bone marrow. J Orthop Res **21:**521–528.
14. **Field JR, McGee M, Stanley R, Ruthenbeck G, Papadimitrakis T, Zannettino A, Gronthos S, Itescu S.** 2011. The efficacy of allogeneic mesenchymal precursor cells for the repair of an ovine tibial segmental defect. Vet Comp Orthop Traumatol **24:**113–121.
15. **Field JR, McGee M, Wildenauer C, Kurmis A, Margerrison E.** 2009. The utilization of a synthetic bone void filler (JAX) in the repair of a femoral segmental defect. Vet Comp Orthop Traumatol **22:**87–95.
16. **Gerber A, Gogolewski S.** 2002. Reconstruction of large segmental defects in the sheep tibia using polylactide membranes. A clinical and radiographic report. Injury **33:**B43–B57.
17. **Gogolewski S, Pineda L, Michael Büsing C.** 2000. Bone regeneration in segmental defects with resorbable polymeric membranes: IV. Does the polymer chemical composition affect the healing process? Biomaterials **21:**2513–2520.
18. **Golub EE, Boesze-Battaglia K.** 2007. The role of alkaline phosphatase in mineralization. Curr Opin Orthop **18:**444–448.
19. **Gregory P, Sanders R**. 1995. The treatment of closed, unstable tibial shaft fractures with unreamed interlocking nails. Clin Orthop Relat Res **315:**48–55.
20. **Gugala Z, Gogolewski S.** 2002. Healing of critical-size segmental bone defects in the sheep tibiae using bioresorbable polylactide membranes. Injury **33 Suppl 2:**B71–B76.
21. **Hahn JA, Witte TS, Arens D, Pearce A, Pearce S.** 2011. Double-plating of ovine critical sized defects of the tibia: a low morbidity model enabling continuous in vivo monitoring of bone healing. BMC Musculoskelet Disord **12:**214.
22. **Högel F, Schlegel U, Südkamp N, Müller C.** 2011. Fracture healing after reamed and unreamed intramedullary nailing in sheep tibia. Injury **42:**667–674.
23. **Liebschner MAK.** 2004. Biomechanical considerations of animal models used in tissue engineering of bone. Biomaterials **25:**1697–1714.
24. **Maissen O, Eckhardt C, Gogolewski S, Glatt M, Arvinte T, Steiner A, Rahn B, Schlegel U.** 2006. Mechanical and radiological assessment of the influence of rhTGFβ-3 on bone regeneration in a segmental defect in the ovine tibia: Pilot study. J Orthop Res **24:**1670–1678.
25. **Marcacci M, Kon E, Zaffagnini S, Giardino R, Rocca M, Corsi A, Benvenuti A, Bianco P, Quarto R, Martin I, Muraglia A, Cancedda R.** 1999. Reconstruction of extensive long-bone defects in sheep using porous hydroxyapatite sponges. Calcif Tissue Int **64:**83–90.
26. **Martini L, Fini M, Giavaresi G, Giardino R.** 2001. Sheep model in orthopedic research: a literature review. Comp Med **51:**292–299.
27. **Mastrogiacomo M, Corsi A, Francioso E, Comite MD, Monetti F, Scaglione S, Favia A, Crovace A, Bianco P, Cancedda R.** 2006. Reconstruction of extensive long bone defects in sheep using resorbable bioceramics based on silicon stabilized tricalcium phosphate. Tissue Eng **12:**1261–1273.
28. **Mills LA, Simpson AH.** 2012. In vivo models of bone repair. J Bone Joint Surg Br **94:**865–874.
29. **Pearce AI, Richards RG, Milz S, Schneider E, Pearce SG.** 2007. Animal models for implant biomaterial research in bone: a review. Eur Cell Mater **13:**1–10.
30. **Peng H, Wright V, Usas A, Gearhart B, Shen HC, Cummins J, Huard J.** 2002. Synergistic enhancement of bone formation and healing by stem cell-expressed VEGF and bone morphogenetic protein 4. J Clin Invest **110:**751–759.

31. **Pluhar GE, Turner AS, Pierce AR, Toth CA, Wheeler DL.** 2006. A comparison of 2 biomaterial carriers for osteogenic protein 1 (BMP7) in an ovine critical defect model. J Bone Joint Surg Br **88:**960–966.
32. **Ralis ZA, Watkins G.** 1992. Modified tetrachrome method for osteoid and defectively mineralized bone in paraffin sections. Biotech Histochem **67:**339–345.
33. **Reichert JC, Epari DR, Wullschleger ME, Saifzadeh S, Steck R, Lienau J, Sommerville S, Dickinson IC, Schütz MA, Duda GN, Hutmacher DW.** 2010. Establishment of a preclinical ovine model for tibial segmental bone defect repair by applying bone tissue engineering strategies. Tissue Eng Part B Rev **16:**93–104.
34. **Reichert JC, Saifzadeh S, Wullschleger ME, Epari DR, Schutz MA, Duda GN, Schell H, van Griensven M, Redl H, Hutmacher DW.** 2009. The challenge of establishing preclinical models for segmental bone defect research. Biomaterials **30:**2149–2163.
35. **Robey PG, Young MF, Flanders KC, Roche NS, Kondaiah P, Reddi AH, Termine JD, Sporn MB, Roberts AB.** 1987. Osteoblasts synthesize and respond to transforming growth factor type β (TGFβ) in vitro. J Cell Biol **105:**457–463.
36. **Rose DM, Smith TO, Nielsen D, Hing CB.** 2013. Expandable intramedullary nails for humeral fractures: a systematic review of clinical and radiological outcomes. Eur J Orthop Surg Traumatol **23:**1–11.
37. **Sarkar MR, Augat P, Shefelbine SJ, Schorlemmer S, Huber-Lang M, Claes L, Kinzl L, Ignatius A.** 2006. Bone formation in a long bone defect model using a platelet-rich plasma-loaded collagen scaffold. Biomaterials **27:**1817–1823.
38. **Skoumal M, Haberhauer G, Kolarz G, Hawa G, Woloszczuk W, Klingler A.** 2005. Serum cathepsin K levels of patients with long-standing rheumatoid arthritis: correlation with radiological destruction. Arthritis Res Ther **7:**R65–R70.
39. **Teixeira CR, Rahal SC, Volpi RS, Taga R, Cestari TM, Granjeiro JM, Vulcano LC, Correa MA.** 2007. Tibial segmental bone defect treated with bone plate and cage filled with either xenogeneic composite or autologous cortical bone graft. An experimental study in sheep. Vet Comp Orthop Traumatol **20:**269–276.
40. **Viateau V, Guillemin G, Yang YC, Bensaid W, Reviron T, Oudina K, Meunier A, Sedel L, Petite H.** 2004. A technique for creating critical-size defects in the metatarsus of sheep for use in investigation of healing of long-bone defects. Am J Vet Res **65:**1653–1657.
41. **Wahl SM.** 1994. Transforming growth factor beta: the good, the bad, and the ugly. J Exp Med **180:**1587–1590.
42. **Yu Y, Yang JL, Chapman-Sheath PJ, Walsh WR.** 2002. TGFβ, BMPs, and their signal transducing mediators, Smads, in rat fracture healing. J Biomed Mater Res **60:**392–397.